



Title	Effects of volume evolution of static and dynamic polar nanoregions on the dielectric behavior of relaxors
Author(s)	Shi, YP; Soh, AK
Citation	Applied Physics Letters, 2011, v. 99 n. 9, article no. 092908
Issued Date	2011
URL	http://hdl.handle.net/10722/157139
Rights	Applied Physics Letters. Copyright © American Institute of Physics.

Effects of volume evolution of static and dynamic polar nanoregions on the dielectric behavior of relaxors

Y. P. Shi and A. K. Soh^{a)}

Department of Mechanical Engineering, The University of Hong Kong, Hong Kong

(Received 23 July 2011; accepted 10 August 2011; published online 2 September 2011)

Recent experiments revealed unusual dielectric behaviors of $\text{Pb}(\text{Mg}_{1/3}\text{Nb}_{2/3})\text{O}_3$ originated from polar nanoregions (PNRs). Thus, Pauli's master equation is adopted to investigate the distinct dielectric responses, correlation strength, and volume evolutions of static and dynamic PNRs. Our findings have not only validated the percolation theory but also ascertained Lorentzian distribution of the rate of thermal change of PNR volume. Finally, based on Maxwell's equation the observed dielectric deviations of bulk permittivity from Curie-Weiss law are attributed to the thermal effects on static volume fraction and polarization rotation. © 2011 American Institute of Physics.

[doi:10.1063/1.3632082]

The physical nature underlying colossal piezoelectric response and broad temperature (T) dielectric dispersion of relaxor ferroelectrics (relaxors) still remains debatable in view of a few controversies between the existing experimental and theoretical results. In contrast to wide acceptability of Curie-Weiss (C-W) relation for the sharp phase transition in normal ferroelectrics, apparent deviations from C-W law have been frequently observed in prototypical relaxors^{1,2} Pirc *et al.*³ found that the deviation that peaked near the Curie-temperature (T_C) was even more significant when a higher electric field (E) was imposed. More and more experiments suggested that unusual relaxor behaviors were closely related to the coexistence and competition between the long-range order and polar nanoregions (PNRs) that appeared below the Burns temperature (T_d). To-date, it is believed that the typical PNRs in relaxors are mutually coupled via interactions with polarizable matrix. In addition to the influence of local PNR polarization,¹ the correlation strength of a "connected" network⁴ composed of high-density PNRs was easily modulated by random fields stemming from structural disorder in multivalent relaxors.³ Recently, Xu *et al.*⁵ have revealed that T - and E -driven redistribution of PNR polarizations played a key role in governing the vagarious dielectric responses of relaxors. Although PNR dynamics in relaxors have been widely studied, some of the observations clearly contradicted the related theories. First, adoption of different nanostructure was unavoidable to interpret the recently observed E -independent source of diffuse scattering intensity.⁵ Second, the latest neutron spin-echo (NSE) measurements⁶ exhibited distinct T -dependence of static and dynamic scattering intensity in $\text{Pb}(\text{Mg}_{1/3}\text{Nb}_{2/3})\text{O}_3$ (PMN) crystals. Furthermore, the following essential problems encountered for clarification of typical relaxor behaviors have yet to be resolved: (i) The methodology for distinguishing different dielectric features of static and dynamic evolution of PNRs and, hence, correlating them with bulk dielectric dispersion and (ii) explanation of the three length scales,⁷ i.e., 5-25 nm sized PNRs, chemical ordering region (COR) of <5 nm, and ferroelastic domain walls (DWs) of

~100 nm in length, which are required for a PMN crystal to stabilize inhomogeneities?

In this letter, these essential issues are addressed to better understand the dielectric behaviors and related properties of relaxors. The total volume of a PNR, V_{total} , can be divided into two components, i.e., a T -dependent static volume (V_{sta}) and a dynamic volume (V_{dyn}) initiated by adequate correlation among PNRs. V_{dyn} is sensitive to T and E in terms of modulation for the interaction strength.

PNRs in PMN have rhombohedral symmetry and [111]-type polarization (with eight easy directions). In general, time (t)-dependent probability (p_n) for PNRs to occupy the n th ground state is governed by Pauli's master equation:^{8,9}

$$\tau \frac{d}{dt} p_n(t) = \sum_{m \neq n} [p_m(t) - e^{U_a} p_n(t)], \quad (1)$$

where integer $n, m \in [1, 8]$ and τ is relaxation time. To further simplify Eq. (1), we restrict it to a two-state system. A generic activation parameter U_a that denotes the energy difference between two ground states is established by combining Néel's proposal⁴ and our recent findings,⁸ i.e., $U_a = QV/kT$, where k is Boltzmann's constant and V is either V_{sta} or V_{dyn} ; Q is the energy density given by $2E|P|^m$, in which $|P|^m$ denotes the PNR polarization maxima. Based on the proposed solution⁹ of Eq. (1), we obtain the bulk PMN polarization magnitude

$$\langle P \rangle = |P|^m \left(\frac{1 - e^{-U_a}}{1 + e^{-U_a}} \right) (1 - e^{-t/\tau}). \quad (2)$$

In order to distinguish the dielectric contributions from V_{sta} and V_{dyn} , it is assumed that V_{sta} has a T -independent polarization maxima, whereas, that of V_{dyn} is the sum of a constant $|P|^m$ and $\varepsilon(T) \times E$, where $\varepsilon(T)$ is T -dependent dielectric permittivity. In the asymptotic limit, substituting Eq. (2) into $\varepsilon(T) = \partial \langle P \rangle / \partial E$ yields the contribution of V_{sta} and V_{dyn} to ε , i.e., ε_{sta} and ε_{dyn}

$$\begin{cases} \varepsilon_{\text{sta}} = \frac{|P|^m}{E} \left(\frac{2U_a}{2 + e^{U_a} + e^{-U_a}} \right) \\ \varepsilon_{\text{dyn}} = \frac{|P|^m}{E} \left(\frac{U_a}{1 - U_a + e^{-U_a}} \right) \end{cases}. \quad (3)$$

^{a)} Author to whom all correspondence should be addressed: Electronic mail: aksoh@hkuc.hku.hk. Tel.: +852-28598061. FAX: +852-28585415.

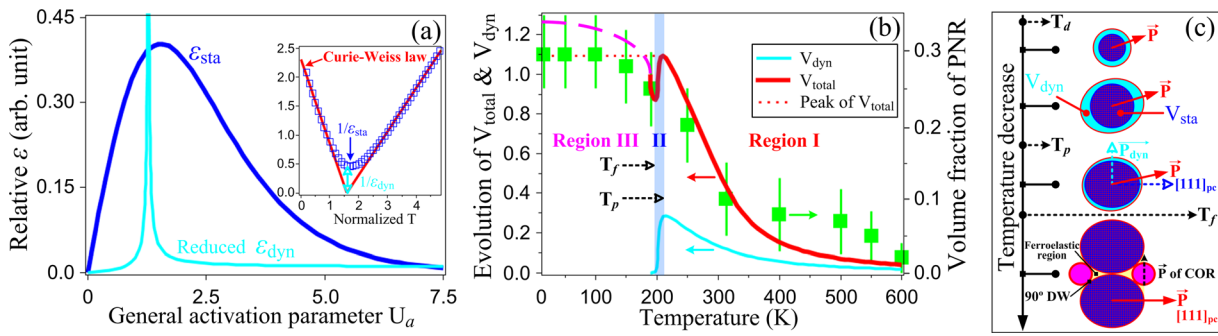


FIG. 1. (Color online) (a) U_a -dependence of ϵ_{sta} and ϵ_{dyn} ; the inset compares $1/\epsilon_{sta}$ and Curie-Weiss law. (b) Comparison of V_{total} and V_{dyn} with the calculated PNR volume fraction (Ref. 10). (c) Schematics for thermal evolutions of V_{sta} and V_{dyn} and rotation of overall polarization (\vec{P}); \vec{P}_{dyn} denotes the polarization direction in V_{dyn} .

The dissimilarity in U_a -dependence of ϵ_{sta} and ϵ_{dyn} shown in Fig. 1(a), represents the distinct dielectric features of V_{sta} and V_{dyn} . ϵ_{sta} disperses over a wide U_a range, whereas ϵ_{dyn} only shows a substantial change near $U_a = 1.278$, at which it diverges in a manner similar to normal ferroelectrics. Furthermore, since the inverse Curie constant ($1/C$) reflects $\partial\epsilon^{-1}/\partial T$, Eq. (3) indicates that the QV/k ratio in relaxors is comparable with the C value. For PMN crystal $Q \sim 2.3 \times 10^{-3} \text{ eV}/(\text{nm})^3$ (Ref. 4) and $C \sim 2.05 \times 10^5 \text{ K}$ (Ref. 7), Eq. (3) predicts a mean volume of $\sim 10^3 \text{ nm}^3$, which tallies with the PNR size of 5-25 nm observed by SEM.⁷

In view of a latest finding⁷ that the C-W relation validates even if T is near T_C , it is postulated that Eq. (3) for local PNRs requires the C-W law to be satisfied. The inset of Fig. 1(a) shows that the $1/\epsilon_{sta}$ given by Eq. (3) is in excellent agreement with the C-W law over a broad T -range, while the minor deviation between them due to the absence of ϵ_{sta} divergence can be eliminated by an appropriate $1/\epsilon_{dyn}$.

The C-W behavior of ϵ_{sta} actually arises from the evolution of V_{total} and V_{dyn} pursuant to the thick and thin curve in Fig. 1(b), respectively. Fig. 1(b) exhibits an outstanding agreement of our predicted V_{total} with the calculated volume fraction of PNRs.¹⁰ Equation (3) underlines the existence of a peak in both the V_{total} and V_{dyn} curve. This suggests that the PNR correlation has both attractive and repulsive feature, and it finally becomes negligible compared with thermal fluctuations. Accordingly, the histogram of PNR evolution is divided into three regions, as depicted in Figs. 1(b) and 1(c). In region I, elliptical PNRs composed of spherical V_{sta} and heterogeneous V_{dyn} , increase gradually while cooling till T_p where all the PNRs percolate through PMN crystal. V_{sta} expands at the expense of V_{dyn} in a narrower region II and it becomes immobile at the freezing temperature (T_f). Mean-

while, a sudden V_{total} decrease and the formation of elliptical V_{sta} would induce profound stresses⁷ due to a higher symmetry of a newly formed V_{sta} than that of V_{dyn} . Finally, in region III, a similar percolation process will take place in the remaining medium, leading to the rebounding of V_{total} [dashed curve in Fig. 1(b)] and formation of smaller CORs.⁷

Another explanation is that the interfacial energies and resultant stresses drive the CORs and V_{sta} self-assembly¹¹ and stabilize long-range order at low temperatures. This may help to explain the observation¹² that PNR/COR was present over a much wider T range in a PMN crystal than in a $\text{Sr}_{1-x}\text{Ba}_x\text{Nb}_2\text{O}_6$ where the stress factor was insignificant. A smaller V_{sta} near T_d should be ineffective for self-stress-relaxation and, thus, formation of a sufficiently large V_{dyn} , e.g., $V_{dyn}/V_{sta} \approx 1$ (Ref. 6) appears inevitable for maintaining the overall cubic symmetry via elimination of stresses. This dynamics is able to redistribute bulk polarization from an initial direction close to [111] easy direction.¹³ Similar to normal ferroelectrics where ferroelastic DWs are involved in minimization of mechanical energy, ferroelastic DWs such as 90° DWs in Fig. 1(c) could also be stabilized to relax the stresses of PNRs, which may be used to explain the measured perpendicularity¹³ of PNR polarization to that of the matrix. Besides, once the dimension of remaining medium is less than a critical size,^{11,14} both high-aspect-ratio DWs and irregular stress field⁷ will appear and persist at low T s.

For explaining the unconventional NSE results,⁶ Fig. 2(a) is plotted, which shows that the V_{sta} curve tallies with the static intensity (SI) when T is decreased from 500 K to 200 K. Besides, before reaching a sudden freezing at 190 K, the V_{sta} curve could be divided into a nearly straight and a nonlinear portion, which agrees with the calculated curve¹ of local order parameter q , as shown in the inset of Fig. 2(a). As

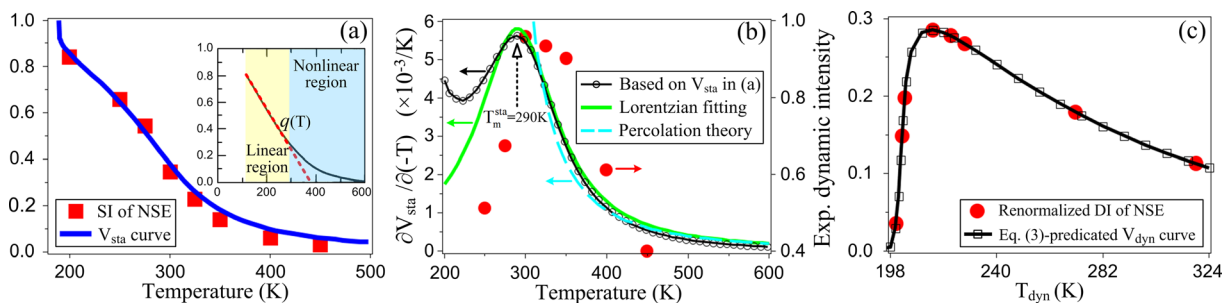


FIG. 2. (Color online) Comparison of (a) the predicted V_{sta} with measured NSR SI data (Ref. 6). The inset displays q vs T calculated in Ref. 1. (b) Variation of $\partial V_{sta}/\partial(-T)$ with the NSE DI (solid circle). (c) Our predicted V_{dyn} with the renormalized DI data; T_{dyn} is the critical temperature to stabilize V_{dyn} .

for the unusual dynamic intensity (DI), we would attribute them to two causes: $\partial V_{\text{sta}}/\partial(-T)$ and variation of V_{dyn} . Intuitively, a larger $\partial V_{\text{sta}}/\partial(-T)$ is bound to augment the measured DI. Hence, $\partial V_{\text{sta}}/\partial(-T)$ is plotted using the V_{sta} data in Fig. 2(a), as shown in Fig. 2(b), in which another two fittings are also displayed. In a mean field case,⁴ percolation theory predicts the PNR mean volume as

$$V = V_0/(1 - T_0/T). \quad (4)$$

The dashed-curve in Fig. 2(b) is a $dV/d(-T)$ fitting based on Eq. (4) with $V_0 \sim 0.1075$ and $T_0 = 243.5$ K, which is close to 224 K given in Ref. 15. Although Pirc and Blinc⁴ assumed that Eq. (4) was valid as long as $T > T_0$, Fig. 2(b) shows that Eq. (4) is only applicable for $T > 315$ K. However, a Lorentzian fitting based on

$$\partial V_{\text{sta}}/\partial(-T) = v_m \vec{T} / \pi \left[(T - T_m^{\text{sta}})^2 + \vec{T}^2 \right] \quad (5)$$

displays an excellent agreement with $\partial V_{\text{sta}}/\partial(-T)$ data down to 250 K. $v_m = 0.369$ and $\vec{T} = 59.12$ K and T_m^{sta} indicate that the rate maxima is at 290 K, which is quite close to the calculated¹ 300 K [refer to Fig. 1(a)]. In general, the relaxor dynamic response is supposed to increase with the growth of V_{dyn} . Thus, the V_{dyn} predicated is also plotted in Fig. 2(c), in which shows perfect agreement with the observed DI data.

Since diffuseness scattering in a cooled relaxor is characterized by a gradual increase in static volume fraction α ,⁶ two mechanisms are proposed to predict the thermal evolution of α . Mechanism I estimates α based on the known V_{total} and V_{sta} [see Figs. 1(b) and 2(a)] as $\alpha_1 = V_{\text{sta}}/V_{\text{total}}$, which yields the solid curve in Fig. 3(a). It can be seen that the decreasing trend of α_1 is similar to that of the experimental data (α_{Exp}).⁶ Instead, mechanism II is based on a thermodynamic stability analysis for a representative PNR. Basically, PNRs can be stabilized by cooling the relaxor from T_d down to a sufficiently low temperature. This is equivalent to that adding V_{dyn} to the already stable V_{sta} requires further cooling the whole PNR to a much lower temperature (T_{dyn}) than T_{sta} to ensure the stability of V_{sta} mechanism II estimates α as

$$\alpha_{\text{II}} = (T_d - T_{\text{sta}})/(T_d - T_{\text{dyn}}), \quad (6)$$

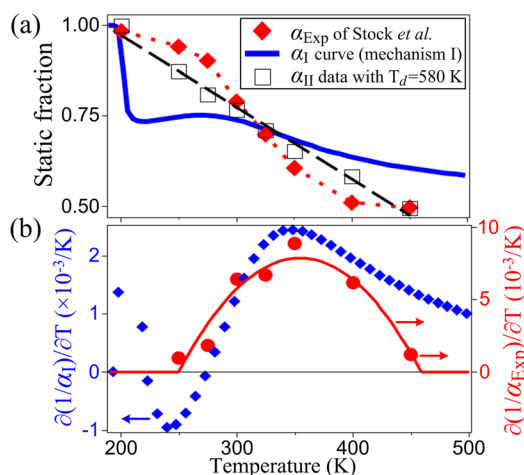


FIG. 3. (Color online) (a) Thermal-evolution of α ; α_{II} is determined from the best fitting of Eq. (6) for α_{Exp} (Ref. 6). (b) Plots of $\partial(1/\alpha_1)/\partial T$ and $\partial(1/\alpha_{\text{Exp}})/\partial T$; the dashed line in (a) and solid curve in (b) is a visual guide.

where T_{sta} and T_{dyn} are the known temperatures of SI and DI data determined in Figs. 2(a) and 2(c). T_d is the only adjustable parameter to our fitting of Eq. (6) for the eight-pair (SI-DI) data. For PMN crystals, the best estimation of T_d is 580 K, which lies in the measured range of 550 K (Ref. 6) to 600 K (Ref. 10).

Lastly, we would correlate the T -dependent α with the thermal dispersion of average permittivity (ϵ_{PNR}) among all the PNRs. For a two-phase dielectric composite,¹⁶ Maxwell's equation predicts that the ϵ_{PNR} satisfies

$$\alpha \left(\frac{1}{3} + \frac{\epsilon_{\text{dyn}}}{\epsilon_{\text{PNR}} - \epsilon_{\text{dyn}}} \right) = \left(\frac{1}{3} + \frac{\epsilon_{\text{dyn}}}{\epsilon_{\text{sta}} - \epsilon_{\text{dyn}}} \right). \quad (7)$$

The symmetric form of Eq. (7) implies that the observed deviation of $1/\epsilon_{\text{PNR}}$ from the C-W law is solely originated from the thermal change of α . Fig. 3(b) shows that $\partial(1/\alpha_1)/\partial T$ and $\partial(1/\alpha_{\text{Exp}})/\partial T$ have similar trend in a broad T -range. Equation (7) infers that the nearly constant α_{Exp} for $T < 249.6$ K and $T > 458.6$ K ensure the obedience of crystal permittivity with the C-W relation, and that dielectric deviation phenomenon can be observed in the middle T -range.

In conclusion, the distinct dielectric responses static and dynamic PNRs are studied based on Pauli's master equation. The PNR correlation is found to peak near the Curie temperature. Two mechanisms have also been proposed to estimate the thermal change of α . Finally, based on Maxwell's equation, the observed deviations of bulk permittivity from the C-W law are attributed to thermal effects on and polarization rotations that occur from T_d to T_f . Our findings are in excellent agreement with the existing theoretical and experimental results.

Research Grants Council of the Hong Kong Special Administrative Region, under Project Nos. HKU 716508E and HKU 717011E, is acknowledged. We thank Prof. G.J. Weng at Rutgers University for helpful discussions.

¹D. Viehland, S. J. Jang, L. E. Cross, and M. Wuttig, *Phys. Rev. B* **46**, 8003 (1992).

²W. Kleemann, J. Dec, V. V. Shvartsman, Z. Kutnjak, and T. Braun, *Phys. Rev. Lett.* **97**, 065702 (2006).

³R. Pirc, R. Blinc, and V. S. Vikhnin, *Phys. Rev. B* **74**, 054108 (2006).

⁴R. Pirc and R. Blinc, *Phys. Rev. B* **76**, 020101(R) (2007).

⁵Z. J. Xu, J. S. Wen, G. Y. Xu, C. Stock, J. S. Gardner, and P. M. Gehring, *Phys. Rev. B* **82**, 134124 (2010).

⁶C. Stock, L. V. Eijck, P. Fouquet, M. Maccarini, P. M. Gehring, G. Y. Xu, H. Luo, X. Zhao, J.-F. Li, and D. Viehland, *Phys. Rev. B* **81**, 144127 (2010).

⁷D. S. Fu, H. Taniguchi, M. Itoh, S.-Y. Koshihara, N. Yamamoto, and S. Mori, *Phys. Rev. Lett.* **103**, 207601 (2009).

⁸Y. P. Shi and A. K. Soh, *Acta Mater.* **59**, 5574 (2011).

⁹M. Vopsaroiu, J. Blackburn, M. G. Cain, and P. M. Weaver, *Phys. Rev. B* **82**, 024109 (2010).

¹⁰I.-K. Jeong, T. W. Darling, J. K. Lee, Th. Proffen, R. H. Heffner, J. S. Park, K. S. Hong, W. Dmowski, and T. Egami, *Phys. Rev. Lett.* **94**, 147602 (2005).

¹¹F. M. Bai, J. F. Li, and D. Viehland, *J. Appl. Phys.* **97**, 054103 (2005).

¹²V. V. Shvartsman, J. Dec, T. Lukasiewicz, A. L. Kholkin, and W. Kleemann, *Ferroelectrics* **373**, 77 (2008).

¹³G. Y. Xu, Z. Zhong, Y. Bing, Z.-G. Ye, and G. Shirane, *Nature Mater.* **5**, 134 (2006).

¹⁴Y. P. Shi, A. K. Soh, and G. J. Weng, *J. Appl. Phys.* **109**, 024102 (2011); Y. P. Shi and A. K. Soh, *EPL* **92**, 57006 (2010).

¹⁵A. Levstik, Z. Kutnjak, C. Filipič, and R. Pirc, *Phys. Rev. B* **57**, 11204 (1998).

¹⁶G. J. Weng, *Mech. Mater.* **42**, 886 (2010).